LA-UR-83-3514

CONF-840647--3

Los Alamos National Laboratory is operated by the University of California for the United States Department of Energy under contract W-7405-ENG-36

LA-UR--83-3514

DE84 004533

TITLE SLIDELINE VERIFICATION FOR MULTILAYER PRESSURE VESSEL AND PIPING ANALYSIS INCLUDING TANGENTIAL MOTION

AUTHOR(S) Leonard A. Van Gulick (Collaborator, Group WX-11)

SUBMITTED TO Paper proposed for presentation at the 1984 ASME Pressure Vessel and Piping Conference, San Antonio, Texas, June 17-21, 1984, and for publication in conference proceedings.

Los Alamos National Laboratory
Los Alamos, New Mexico 87545

SLIDELINE VERIFICATION FOR MULTILAYER PRESSURE VESSEL AND PIPING ANALYSIS INCLUDING TANGENTIAL MOTION

by

Leonard A. Van Gulick, Collaborator
Los Alamos National Laboratory
Los Alamos, New Mexico

Nonlinear finite element method (FEM) computer codes with slideline algorithm implementations should be useful for the analysis of prestressed multilayer pressure vessels and piping. This paper presents closed form solutions including the effects of tangential motion useful for verifying slideline implementations for this purpose. The solutions describe stresses and displacements of a long internally pressurized elastic-plastic cylinder initially separated from an elastic outer cylinder by a uniform gap. Comparison of closed form and FEM results evaluates the usefulness of the closed form solution and the validity of the slideline implementation used.

NOMENCLATURE

a,b	inner and outer radii, inner cylinder
c,d	inner and outer radii, outer cylinder
C,C_1,C_2	boundary condition dependent constants
E_1,E_2	Young's modulus, inner, outer cylinders
K_1,K_{11}	stiffness parameters, inner cylinder
K_2	stiffness parameter, outer cylinder
K_3	combined stiffness parameter
p	internal pressure, inner cylinder
p_4^*	limiting pressure for separation
p_I	interface pressure
r	radius
u	displacement, outer surface, inner cylinder
β_1,β_2	thickness ratio, inner, outer cylinders
Δp	internal pressure decrease
Δp_I	interface pressure decrease
μ_1,μ_2	Poisson's ratio, inner, outer cylinders
σ_θ	hoop stress, inner cylinder
σ_r	radial stress, inner cylinder
$\sigma_r^E,\sigma_\theta^E$	elastic unloading stresses
σ_y	yield stress, inner sphere
σ_{ym}	modified yield stress, inner sphere

Subscripts Denote Quantities Associated With:

1	initial yielding
2	complete yielding
3	gap closure
4	peak pressurization
5	separation
6	complete pressure release
7	operating conditions

INTRODUCTION

The recent development and implementation in nonlinear finite element method (FEM) computer codes of slideline algorithms (1,2) should facilitate the inclusion of the effects of initial interlayer gaps in the analysis of prestressed multilayer pressure vessels and piping being developed for commercial nuclear reactors (3). Verification of the ability of FEM codes to carry out this analysis has been limited, however, by a scarcity of appropriate closed form solutions to which code results could be compared. Needed are closed form solutions for stresses and displacements for problems that include initiation and termination of interlayer contact, tangential or "sliding" motion of contacting surfaces, and plastic material behavior followed by elastic unloading and subsequent reloading.

Closed form solutions for two internally pressurized concentric spheres initially separated by a uniform gap have been found useful for partially verifying slideline implementations (4). Lack of tangential motion, however, due to the spherically symmetrical geometry prevents use of these solutions to evaluate code ability to correctly describe sliding motion.

This study develops closed form solutions that include tangential motion suitable for slideline verification. The problem treated consists of two long, concentric, thick-walled, open-ended cylinders subjected to internal pressure. The two cylinders are initially separated by a uniform gap large enough to allow complete yielding of the inner cylinder before it contacts the outer one. Contact between the two cylinders is assumed to be frictionless, permitting sliding or tangential axial motion to occur between them after contact, as well as before. Elastic-perfectly plastic material behavior for the inner cylinder and elastic behavior for the outer cylinder are assumed. A pressure-time history consisting of initial pressurization, pressure release, and repressurization to operating pressure is considered.

Closed form results for an arbitrary choice of geometry and pressure levels are compared to FEM results obtained using ADINA (5,6) and a recently implemented slideline algorithm (7). The comparison leads to an evaluation of the value of the closed form solutions for slideline verification and of the validity of the particular slideline implementation used.

CLOSED FORM FORMULATION

Equations for the stresses and displacements in a long elastic, thick-walled, open-ended cylinder, subjected to internal and external pressures are readily available (8). Standard plasticity texts (9,10) describe the behavior of a long thick-walled elastic-plastic cylinder subjected to internal pressure. These results can be combined and extended to treat multilayer cylindrical configurations (11). This procedure was used to develop closed form solutions for stresses and displacements in the two cylinders with inner and outer radii, a, b, and c, d, shown in Fig. 1.

The pressure-displacement diagram shown in Fig. 2 relates the displacement of the outer surface of the inner cylinder to internal pressure during initial pressurization to peak pressure, p_4, pressure release, and repressurization to operating pressure, p_7. As shown, separation may or may not occur during pressure release depending on the peak pressure chosen.

The slope of the preyield portion of the curve is determined by the stiffness of the inner cylinder.

$$K_1 = \frac{E_1}{2b_1} (\beta_1^2 - 1) \tag{1}$$

where

$$\beta_1 = b/a \tag{2}$$

and E_1 is Young's modulus for the inner cylinder.

The pressure at which yielding begins, p_1, determined using the Tresca yield criterion, and the corresponding displacement, u_1, are

$$p_1 = \frac{1}{2} \frac{(\beta_1^2 - 1)}{\beta_1^2} \sigma_y \tag{3}$$

$$u_1 = \frac{b\sigma_y}{\beta_1^2 E_1} \tag{4}$$

where σ_y is the yield stress for the inner cylinder.

Yielding completely through the wall of the inner cylinder occurs at a pressure, p_2, and produces a displacement, u_2,

$$p_2 = \sigma_y \ln \beta_1 \tag{5}$$

$$u_2 = \frac{b\sigma_y}{E_1} \left(1 - \mu_1^2 + 2\mu_1^2 \frac{\ln \beta_1}{\beta_1^2 - 1}\right) \tag{6}$$

where μ_1, is Poisson's ratio for the inner cylinder.

Unrestrained expansion at constant pressure occurs from 2 to 3. The displacement at 3, u_3, is the initial gap.

$$u_3 = c - b \tag{7}$$

The slope of the remainder of the loading curve, K_2, is determined by a stiffness parameter relating displacement of the internal surface of the outer cylinder, with Young's modulus, E_2, and Poisson's ratio, μ_2, to interface pressure, p_I.

$$K_2 = \frac{E_2}{c}\,\frac{(\beta_2^2-1)}{(\beta_2^2+1)+\mu_2(\beta_2^2-1)} \tag{8}$$

The thickness ratio of the outer cylinder is

$$\beta_2 = d/c \tag{9}$$

Maximum displacement, u_4, occurs at peak pressure, p_4,

$$u_4 = u_3 + \frac{(p_4-p_2)}{K_2} \tag{10}$$

The two cylinders unload elastically as an integral unit when pressure release begins. Their combined stiffness, K_3, determines the initial slope of the unloading curve,

$$K_3 = \frac{K_1(K_{11}-K_2)}{K_{11}} \tag{11}$$

where K_{11} is the stiffness parameter relating the displacement at the outer surface of the inner cylinder to a change in interface pressure.

$$K_{11} = -\frac{E_1}{b}\,\frac{(\beta_1^2-1)}{(\beta_1^2+1)-\mu(\beta_1^2-1)} \tag{12}$$

Separation will occur if the outer cylinder reaches its undeformed position. The interface pressure will then be zero and the inner cylinder will move in alone, with additional displacements related to further reductions in internal pressure by the original stiffness, K_1. The separation pressure, p_5,

$$p_5 = p_4 - \frac{K_3}{K_2}(p_4 - p_2) \tag{13}$$

is physically meaningful only if positive. Negative values indicate complete pressure release without separation and are associated with peak pressures greater than a limiting value, p_4^*.

$$p_4^* = \frac{K_3 p_2}{K_3 - K_2} \tag{14}$$

A residual displacement, u_6, exists when the initial pressure is fully released.

$$u_6 = u_3 - p_5/K_1 \qquad p_4 \leq p_4^* \tag{15}$$

$$u_6 = u_4 - p_4/K_3 \qquad p_4 \geq p_4^* \tag{16}$$

Repressurization to operating pressure, p_7, produces elastic behavior described by proceeding back up along the unloading curve.

Radial and hoop stresses at radius, r, in the inner cylinder after yielding reaches its outer surface are given by

$$\sigma_r = \sigma_y \ln\left(\frac{r}{a}\right) + C \tag{17}$$

$$\sigma_\theta = \sigma_r + \sigma_y \tag{18}$$

with C a boundary condition dependent constant.

Peak stresses are found by setting $r=a$, $\sigma_r=-p_4$, and solving for C.

$$\sigma_{4r}=\sigma_y \ln\left(\frac{r}{a}\right)-p_4 \tag{19}$$

$$\sigma_{4\theta}=\sigma_y\left(1+\ln\left(\frac{r}{a}\right)\right)-p_4 \tag{20}$$

The maximum interface pressure, p_{I4}, is found by substituting $r=b$ into eqn. (19).

$$p_{I4}=p_4-\sigma_y \ln\beta_1=p_4-p_2 \tag{21}$$

Inner cylinder stresses during pressure release are obtained by superimposing on the peak stresses a system of elastic stresses,

$$\sigma_r^E=C_1+\frac{C_2}{r^2} \tag{22}$$

$$\sigma_\theta^E=C_1-\frac{C_2}{r^2} \tag{23}$$

with constants evaluated using boundary conditions, $\sigma_r^E=\Delta p$ and $\sigma_r^E=\Delta p_I$, at $r=a$ and $r=b$.

Residual stresses at complete pressure release, $\Delta p=p_4$, are found using $\Delta p_I=p_{I4}$ when separation occurs and $\Delta p_I=K_2p_4/K_3$ when it does not.

$$\sigma_{6r}=\sigma_y\left(\ln\left(\frac{r}{a}\right)-\frac{\beta_1^2}{\beta_1^2-1}\ln\beta_1\left(1-\left(\frac{a}{r}\right)^2\right)\right) \tag{24}$$

$$\sigma_{6\theta}=\sigma_y\left(1+\ln\left(\frac{r}{a}\right)-\frac{\beta_1^2}{\beta_1^2-1}\ln\beta_1\left(1+\left(\frac{a}{r}\right)^2\right)\right) \tag{25}$$

For $p_4 \le p_4^*$ (separation)

$$\sigma_{6_r} = \sigma_y \ln\left(\frac{r}{a}\right) - p_4 \frac{\beta_1^2}{\beta_1^2 - 1}\left(1 - \left(\frac{a}{r}\right)^2\right)\left(1 - \frac{K_2}{K_3}\right) \tag{26}$$

$$\sigma_{6_\theta} = \sigma_y \left(1 + \ln\left(\frac{r}{a}\right)\right) - p_4 \frac{\beta_1^2}{\beta_1^2 - 1}\left(1 + \left(\frac{a}{r}\right)^2\right)\left(1 - \frac{K_2}{K_3}\right) \tag{27}$$

For $p_4 \ge p_4$ (no separation)

Contact is assumed after repressurization to operating pressure, p_7. The operating stresses, σ_{7_r}, and σ_{7_θ} are found by substituting $\Delta p = p_4 - p_7$ and $\Delta p_i = K_2 \Delta p / K_3$ into (22) and (23) and adding the resulting stress system to the peak stresses.

$$\sigma_{7_r} = \sigma_y \ln\left(\frac{r}{a}\right) - p_4$$

$$+ (p_4 - p_7) \frac{1}{\beta_1^2 - 1}\left(\frac{K_2}{K_3}\left(1 - \left(\frac{a}{r}\right)^2\right)\beta_1^2 - \left(1 - \beta_1^2 \left(\frac{a}{r}\right)^2\right)\right) \tag{28}$$

$$\sigma_{7_\theta} = \sigma_y \left(1 + \ln\left(\frac{r}{a}\right)\right) - p_4$$

$$+ (p_4 - p_7) \frac{1}{\beta_1^2 - 1}\left(\frac{K_2}{K_3}\left(1 + \left(\frac{a}{r}\right)^2\right)\beta_1^2 - \left(1 + \beta_1^2 \left(\frac{a}{r}\right)^2\right)\right) \tag{29}$$

FINITE ELEMENT METHOD CALCULATIONS

ADINA is a general purpose, nonlinear finite element method structural analysis code into which a slideline algorithm that uses constraint equations based on the work of Taylor, Hughes, et al. (12) has been introduced. Contact compatibility is imposed by Lagrange multiplier techniques, with the multipliers representing nodal contact forces.

ADINA calculations were carried out for an arbitrarily chosen set of dimensions and material properties for which $b/a=1.25$, $c/a=1.252$, $d/a=1.50, E_1=E_2$, $\mu_1=\mu_2=.3$, and $\sigma_y=1\times10^{-3}E_1$.

The axisymmetric finite element model used in the calculations is shown in Fig. 3. A frictionless interface between the two cylinders was specified, permitting axial sliding or tangential relative motion of the contacting surfaces. The model has 2222 node points and 2000 four node elements. The contacting surfaces are each defined by 101 node points.

Calculations were carried out in a stepwise fashion because of the ADINA incremental solution scheme. A loading sequence of sixteen steps and an unloading sequence of twenty steps were used, with operating stresses determined during unloading. Much smaller steps were used in those portions of the calculations during which contact was initiated or terminated than were used elsewhere. No concerted effort was made to minimize the number of steps.

Equilibrium iteration was carried out at each load step and the stiffness matrix was reformulated as well. The Newton Raphson method was used to solve the incremental equilibrium equations. The ADINA material nonlinearity only analysis option was chosen because of the small displacements and strains associated with the subject problem. Averaging of Gauss point values to define element stresses was carried out as part of the postprocessing procedure.

The inner cylinder was modeled with ADINA material model eight, elastic-plastic with a von Mises yield criterion and isotropic hardening. The tangent modulus was specified as $1\times10^{-3}E$, rather than zero, to avoid possible numerical difficulties associated with a singular inner cylinder stiffness matrix following complete yield and prior to contact. Supplementary calculations showed results to be quite insensitive to tangent modulus, as long as it was small compared to Young's modulus.

NUMERICAL RESULTS AND CONCLUSIONS

Distributions through the inner cylinder wall of nondimensionalized peak, residual and operating stresses are presented in Figs. 4 through 9 for $p_4 = .3\sigma_y$ and $p_7 = .2\sigma_y$. Closed form results were computed with a modified yield stress, σ_{ym},

$$\sigma_{ym} = \left(\frac{4\beta_1^4}{3\beta_1^4 + 1}\right)^{\frac{1}{2}} \sigma_y \tag{30}$$

chosen to partially compensate for the different yield criteria, Tresca and von Mises, used in the closed form and FEM calculations.

Excellent agreement is seen to exist between closed form and FEM results, even for residual stress calculations, which pose a severe test for slideline algorithms. Note that both closed form and FEM results for residual radial stresses, σ_{7_r}, are very small throughout the cylinder wall. Separation following pressure release is indicated by the zero residual radial stress at the contact surface, r/a=1.25. This is as expected, since p_4 was chosen less than p_4^* in order to test the algorithm's ability to correctly describe surface separation during unloading.

The closed form results developed are seen to be useful for verifying FEM slideline implementations. Algorithm ability to correctly describe the initiation and termination of contact between frictionless sliding surfaces of elastic-plastic pressure vessels and piping can be verified using these results. The ADINA slideline implementations used can be considered at least partially verified for computations of this type.

FIGURES

REFERENCES

1. Hallquist, J.O., "A Numerical Treatment of Sliding Interfaces and Impact," AMD-Vol. 30, Computational Techniques for Interface Problems, Park, K.C. and Gartling, D. eds., American Society of Mechanical Engineers, 1978.

2. _________, "NIKE2D: An Implicit, Finite Deformation, Finite Element Code for Analyzing the Static and Dynamic Response of Two Dimensional Solids," Lawrence Livermore Laboratory Report UCRL-52678, 1979, University of California, Livermore, Calif.

3. Uber, G.F. and Langford, P.J., "Analysis of Prestressed Double Wall Tubing for LMFBR Steam Generators," ASME Paper No. 81-PVP-25, American Society of Mechanical Engineers, 1981.

4. Van Gulick, L.A., "Slideline Verification for Multilayer Pressure Vessel and Piping Analysis," ASME Paper No. 83-PVP-28, American Society of Mechanical Engineers, 1983.

5. Bathe, K.J., "Static and Dynamic Geometric and Material Nonlinear Analysis Using ADINA," Report 82448-2, Rev. 1977, M.I.T. Department of Mechanical Engineering, Acoustics and Vibrations Laboratory, Cambridge, Mass.

6. _________, "ADINA-A Finite Element Program for Automatic Dynamic Incremental Nonlinear Analysis," Report 82488-1, Rev. 1978, M.I.T.

Department of Mechanical Engineering, Acoustics and Vibrations Laboratory, Cambridge, Mass.

7. Guerra, F.M., and Browning, R.V., "Comparison of Two Slideline Methods Using ADINA," Computers and Structures, Vol. 17, No. 5-6, 1983, pp. 819-834.

8. Roark, R.J., and Young, W.D., Formulas for Stress and Strain, 5th ed., McGraw-Hill, New York, 1975, pp. 504-506.

9. Mendelson, A., Plasticity: Theory and Application, 1st ed., Macmillan, New York, 1968, pp. 135-148.

10. Hoffman, O., and Sachs, G., Introduction to the Theory of Plasticity for Engineers, 1st ed., McGraw-Hill, New York, 1953, pp. 69-78.

11. Pai, D.H., and Berman, I., "Two-Layer Vessel Fabrication by Pressurization-Theory and Experiment," ASME Paper No. 66-PVP, American Society of Mechanical Engineers, 1966.

12. Hughes, T.J.R. et al., "Finite Element Models for Large Displacement Contact-Impact Analysis," 76-4, July 1976, Dept. of Civil Engineering, University of Calif., Berkeley, Calif.

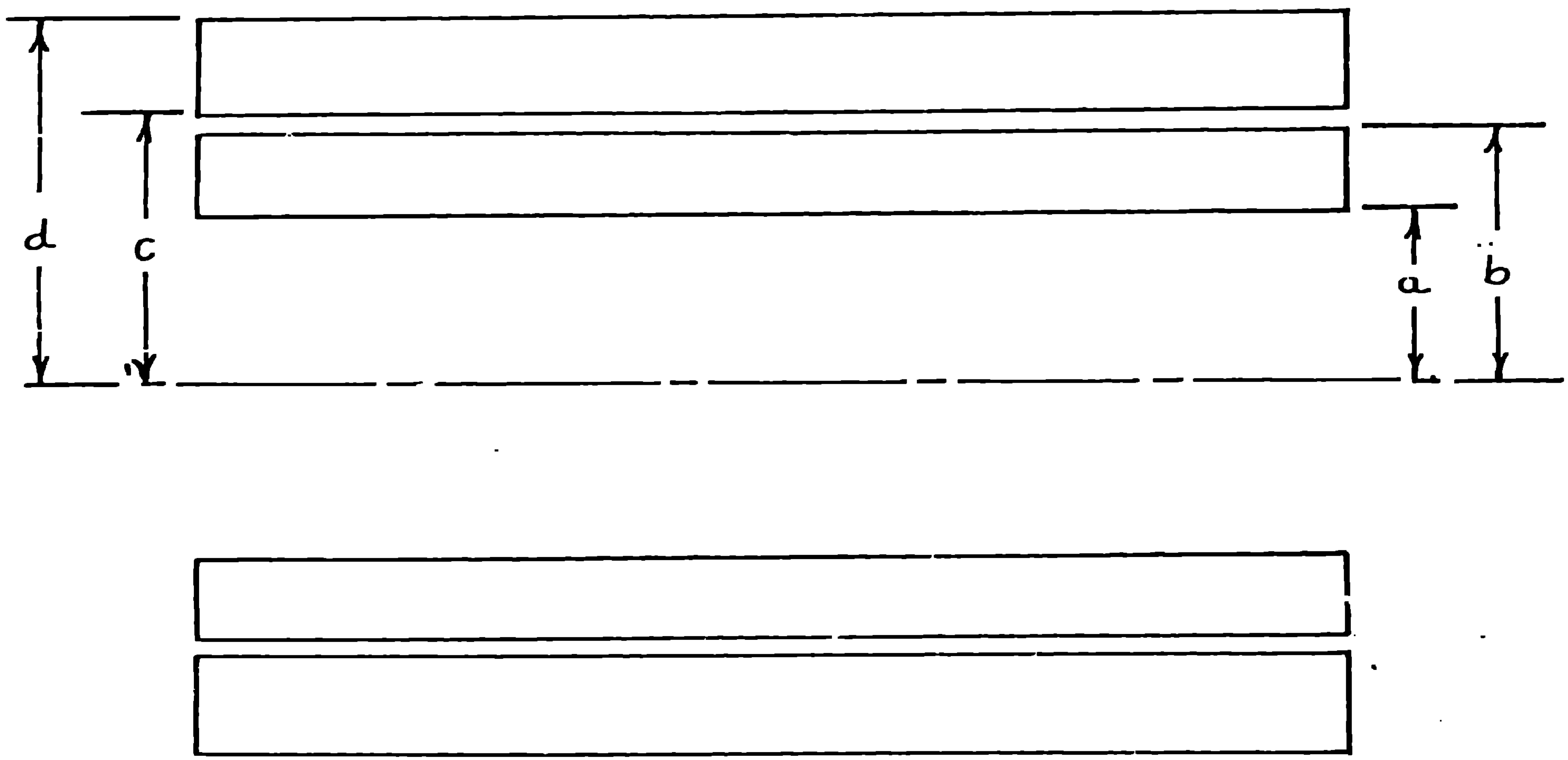

FIGURE 1

FIGURE 2

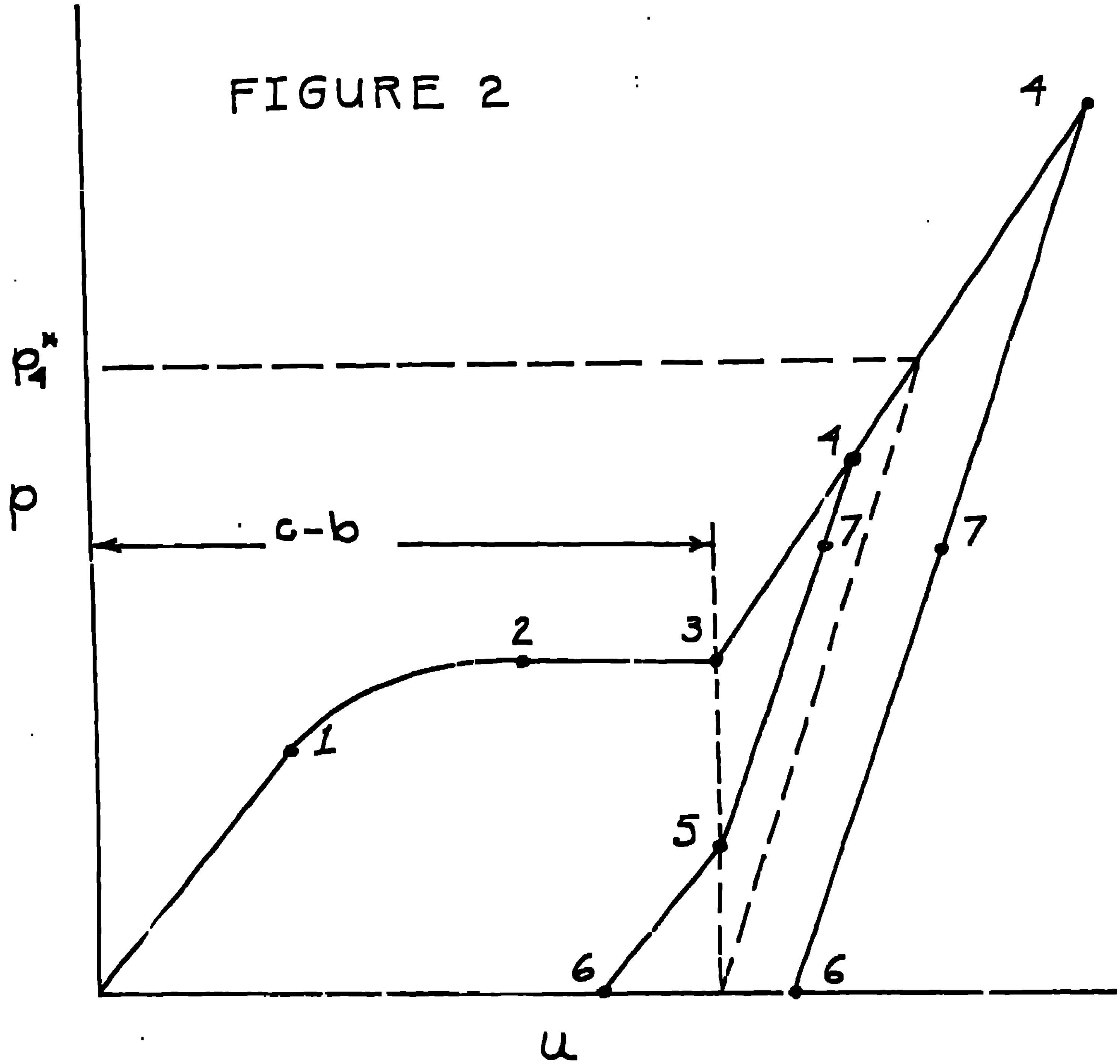

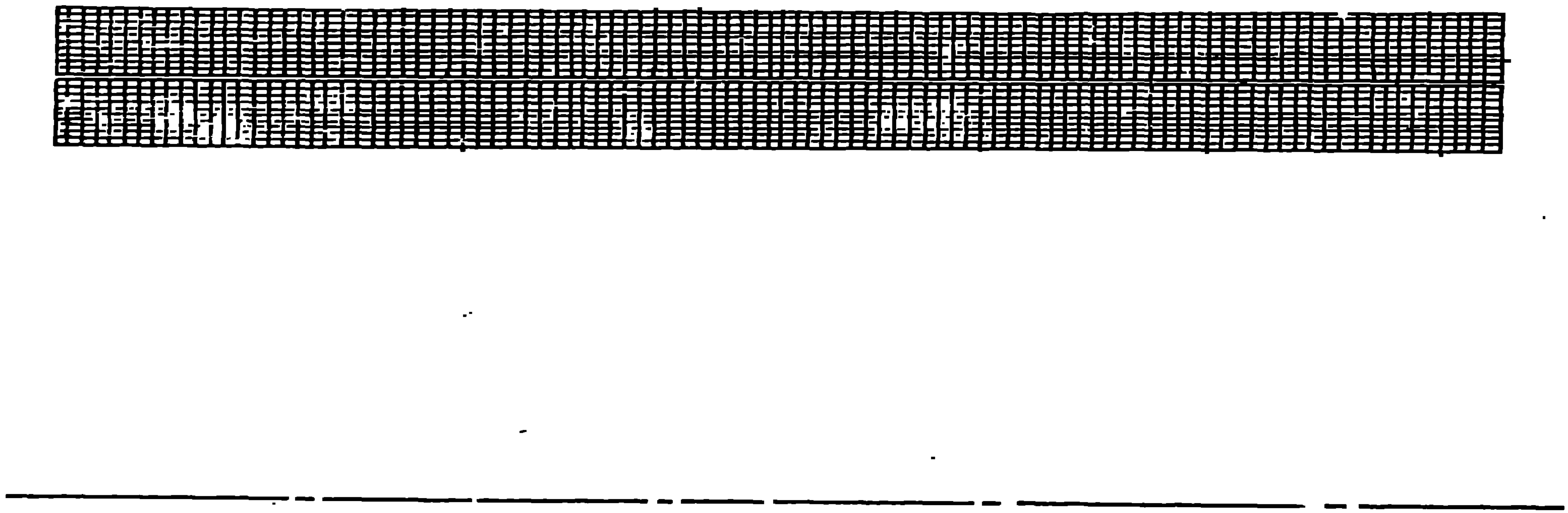

FIGURE 3

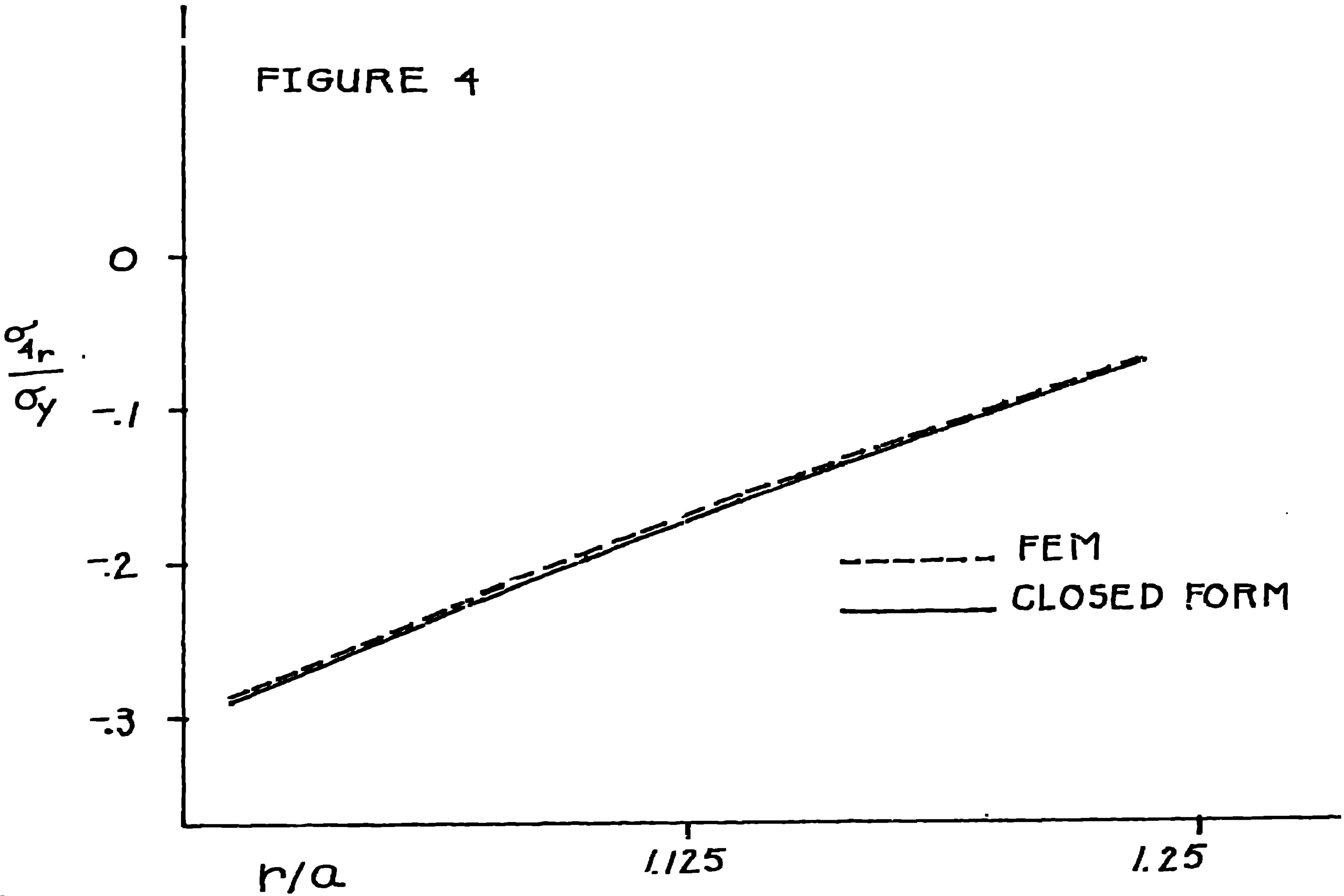

FIGURE 4
0
-.1
-.2
-.3
$\frac{\sigma_{4r}}{\sigma_y}$
FEM
CLOSED FORM
r/a
1.125
1.25

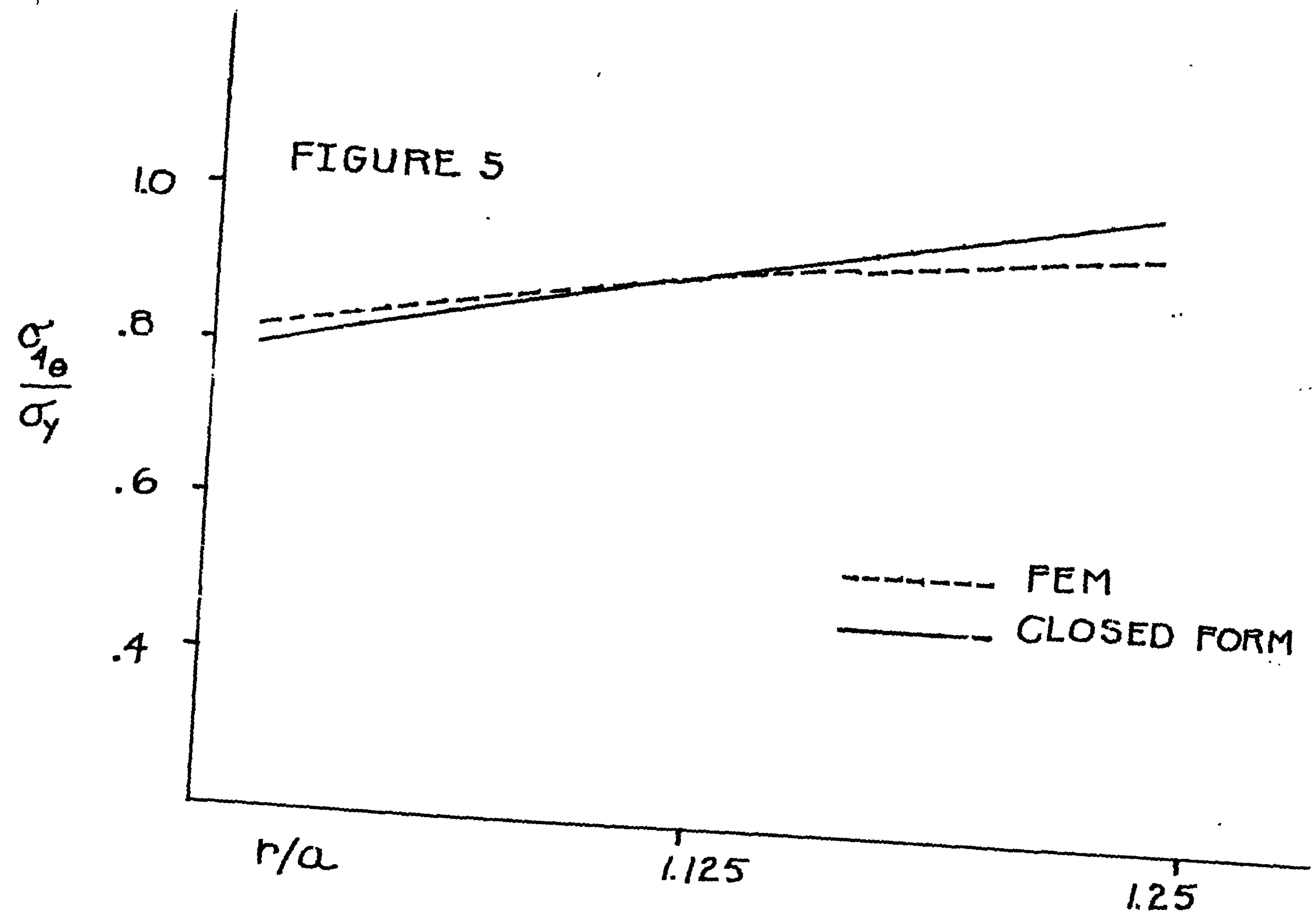

FIGURE 5
1.0
.8
.6
.4
$\frac{\sigma_{1\theta}}{\sigma_y}$
FEM
CLOSED FORM
r/a
1.125
1.25

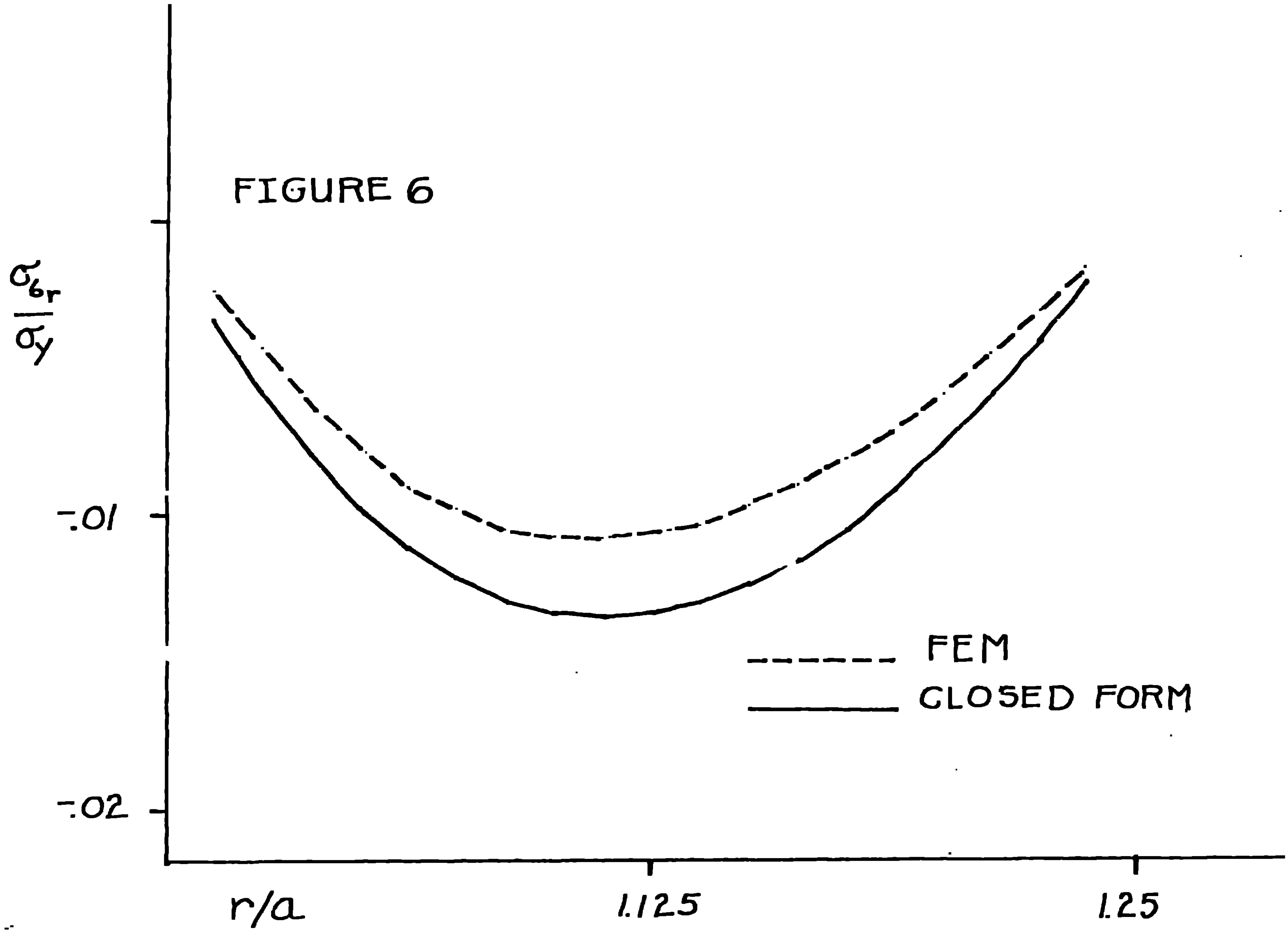
FIGURE 6
$\frac{\sigma_{6r}}{\sigma_y}$
-.01
-.02
FEM
CLOSED FORM
r/a
1.125
1.25

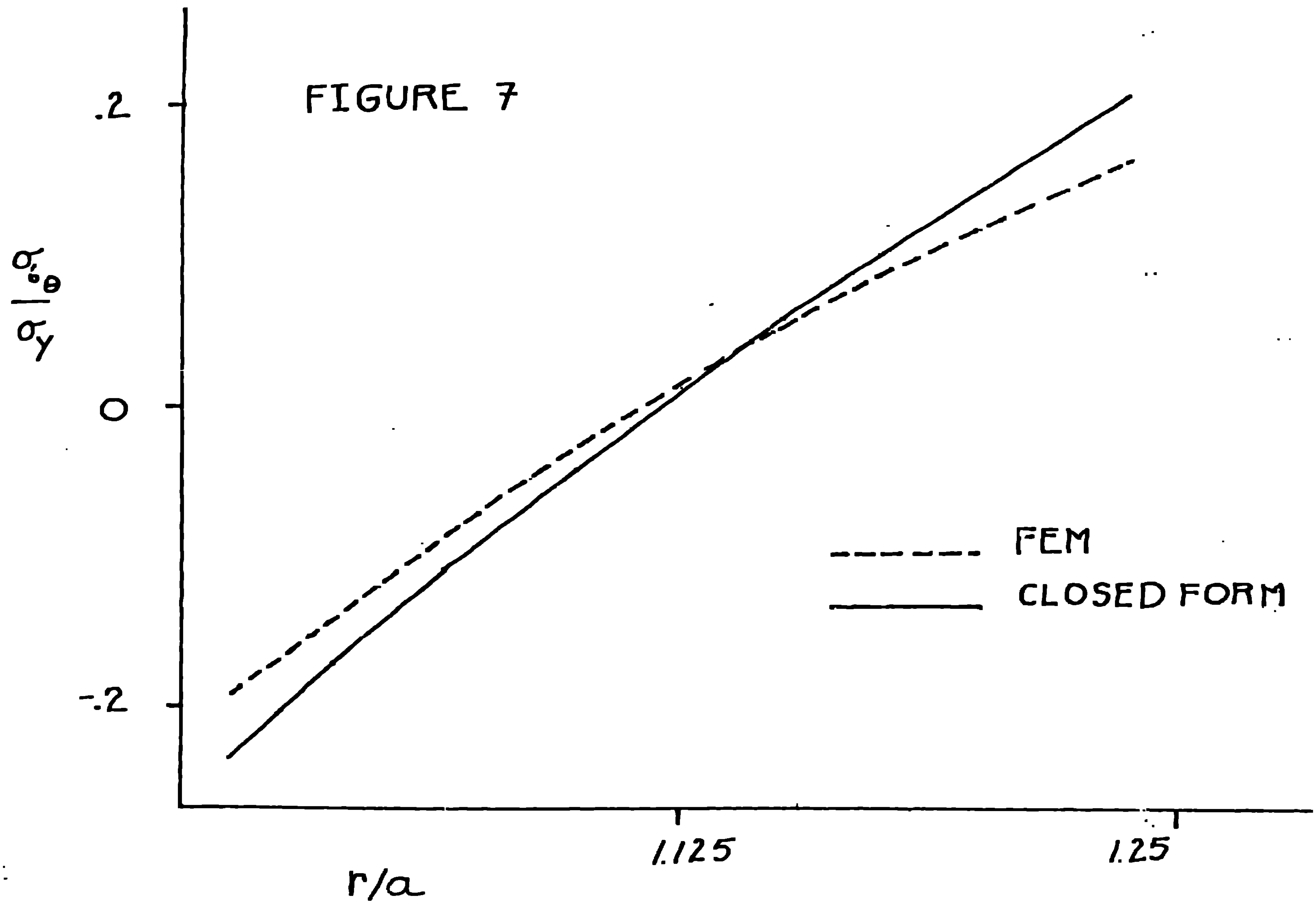
FIGURE 7
.2
0
-.2
$\frac{\sigma_\theta}{\sigma_y}$
FEM
CLOSED FORM
1.125
1.25
r/a

FIGURE 8

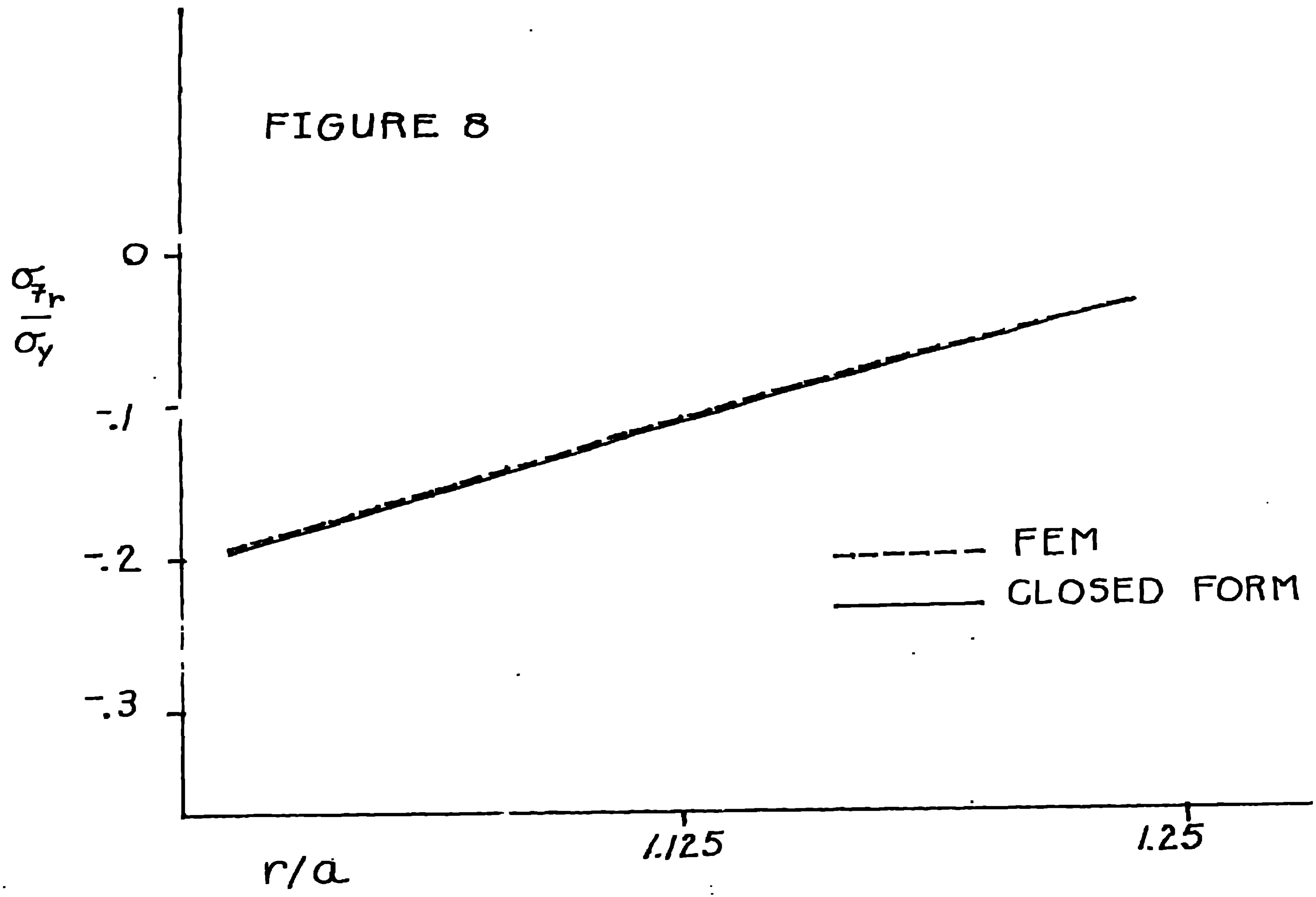

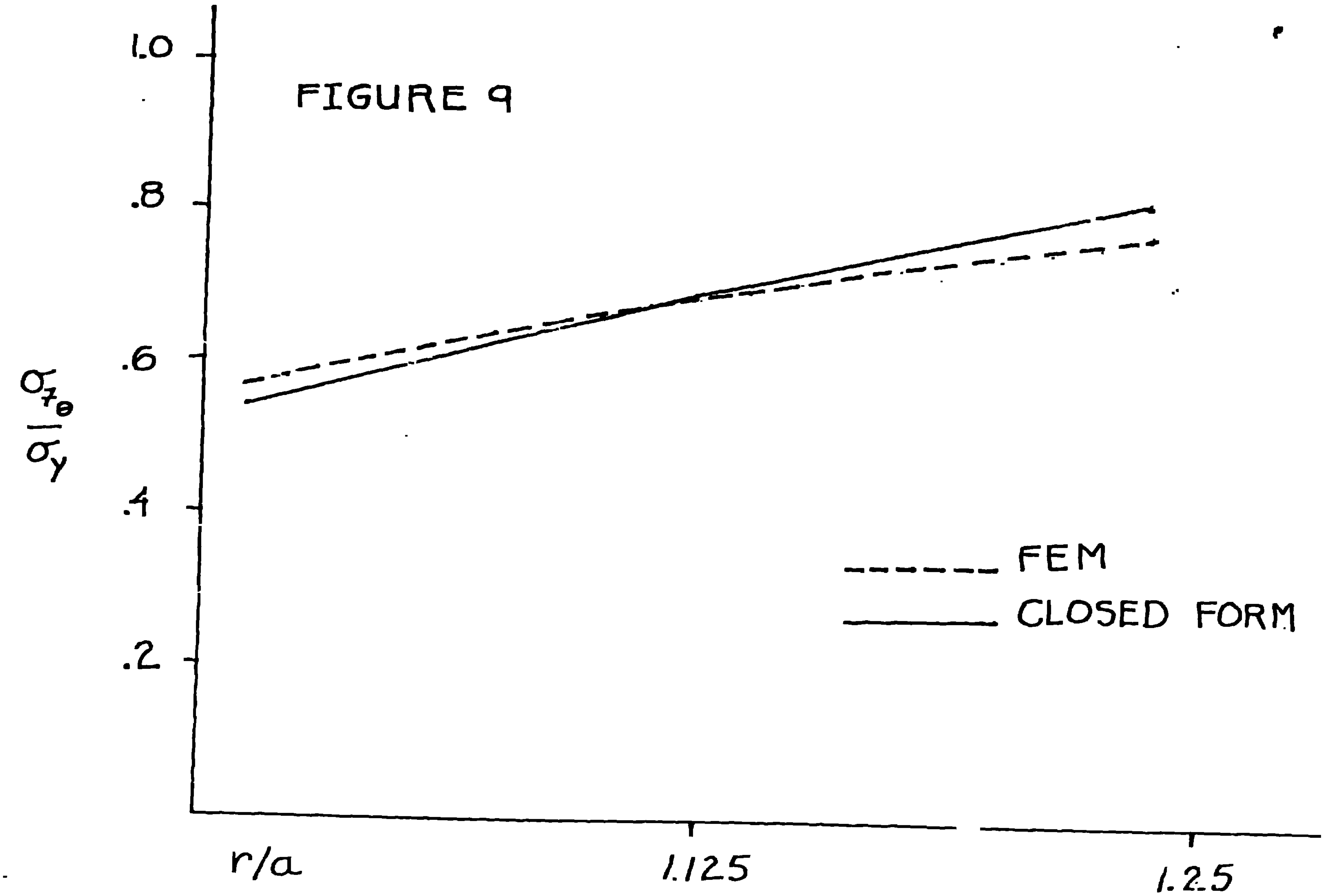

FIGURE 9